DOI: 10.21062/mft.2025.045 http://www.journalmt.com

Surface Treatment of Nylon Filters with Thin Layers of Ti, Cu, and Zr Metals and AgCu Alloys using PVD Magnetron Sputtering Technology

Anna Krobotová (0009-0001-8148-5120)[1], Totka Bakalova (0000-0003-2617-0473)[1], Michal Krafka (0000-0003-3928-6889)[1], Magdalena Mrózek (0009-0001-7144-5897)[1], Lucie Svobodová (0000-0001-8661-5150)[1], Pavel Kejzlar (0000-0002-1323-6114)[1], Blanka Tomková (0000-0002-1301-6533)[2]
[1]Faculty of Mechanical Engineering, Technical University of Liberec, Studentská 2, 461 17 Liberec, Czech Republic. E-mail: anna.krobotova@tul.cz, totka.bakalova@tul.cz, michal.krafka@tul.cz, magdalena.mrozek@tul.cz, lucie.svobodova@tul.cz, pavel.kejzlar@tul.cz
[2]Faculty of Textiles, Technical University of Liberec, Studentská 2, 461 17 Liberec, Czech Republic. E-mail: blanka.tomkova@tul.cz

The development and characterizing of thin layers of AgCu, Cu, Ti, and Zr on nylon filters using PVD magnetron sputtering technology was conducted. The evaluation of these thin layers was mainly focused on characterizing specific parameters that may influence the expected functionality of the modified filter materials. The surface treatment of nylon filters with thin layers does not significantly affect the mechanical properties of the original nylon material. Thin layers deposited at a power of 0.9 kW exhibited greater thickness and lower static friction coefficient values than the layers deposited at 0.4 kW, except for a thin layer of the element titanium. The surface modification of the filters did not significantly change resistance to deformation and had no significant reduction in pore size. However, a significant effect on surface wettability (increased hydrophobicity) was demonstrated.

Keywords: AgCu, Cu, Ti, Zr, Thin Layers, PVD, Magnetron Sputtering, Nylon Filters, Filtration, Functional Properties

1 Introduction

In recent years, there has been increasing attention on improving the properties of filtration materials for various industrial applications. Nylon filtration materials are widely used due to their high mechanical strength, chemical resistance, and good permeability. Improving filter features (e.g., lifespan, utility properties) is crucial for applications requiring high levels of cleanliness and reliability, such as the pharmaceutical industry, food processing, or biotechnology. [1–3] One promising method for modifying the surface of nylon filtration materials is magnetron sputtering. This technique allows the deposition of thin layers of various materials onto the substrate surface using a plasma process. DC (Direct Current) high-vacuum magnetron sputtering uses deposition temperatures close to room temperature and ensures good adhesion of the sputtered layers to the substrate (high fixation efficiency to the base). This technology is also used to apply thin layers that provide antibacterial properties to the modified surface. Elements such as copper, silver, or a mixture of copper and silver can be used to create layers. [2–5]; currently, they are used to create antibacterial surfaces for the food packaging industry, medical devices such as prostheses and catheters, textile surfaces (e.g., healthcare equipment), and more. [6] Trends and innovations in filtration technology applications for various uses (particle separation, medicine, pharmaceuticals, air, and water purification) are also being explored, with the possibility of application to various types of filters (non-woven fabrics, various types of fibres, polymers, glass, etc.). [7, 8]

Copper is a more suitable alternative to silver because it is more affordable, and its residual traces are more easily released from the human body. Studies have monitored the antibacterial effects of different thicknesses of silver and copper thin layers and combinations of both elements (multilayers), revealing similar results in combating bacteria. The proposed surface modifications of the filter materials were investigated before and after exposure to contaminated water; in both cases, good adhesion of the layers to the fibrous substrates was observed. [3, 5]

The presented research focuses on optimizing the deposition parameters and the possibility of combining the elements Cu and Ag in thin layers on flexible filtration materials using magnetron deposition at low temperatures. The aim is to evaluate the influence of different plasma process deposition parameters on the surface layers properties and their impact on filtration rate and material utility properties while maintaining the functional properties of the original material.

2 Experimental procedure

2.1 Materials used and sample preparation

AgCu, Cu, Ti, and Zr thin layers were deposited on nylon membrane filters from the company Fisherbrand, with a diameter of 47 mm, thickness of 150-187 μm, and porosity of 0.45 μm. These filters, from Polyamide 6.6 (nylon), are used for aqueous solutions and most organic solvent filtration. Their main properties include hydrophilicity, wet strength, and dry strength. [9]

To evaluate the functional properties of the modified materials, whole filters were used, or filters were cut to the required sizes for specific tests. For tribological analysis and drop test, the filters were cut in half and attached to microscope slides with double-sided adhesive tape. For resistance to deformation evaluation, the filters were cut to the required size (described in chapter 2.7).

2.2 Thin layers preparation

Thin layers were deposited by DC magnetron sputtering in the coating device NP 70 (KWS s.r.o.) using targets of copper-silver alloy (AgCu, element ratio of Ag 58 at. % and Cu 42 at. %), Copper (99.9 at. %), Titanium (99.5 at. %), Zirconium (99.5 at. %). The distance of the filter material samples from the target during the disposition process was 120 mm.

The deposition was under the following technological conditions: chamber pressure of 0.13 Pa, argon as a working gas, and a deposition time corresponding to 3 rotations of the table (10 °/sec). The thin layers were created from targets of zirconium, copper, titanium, and a copper-silver alloy with a composition of 30 wt. % Cu and 70 wt. % Ag. The samples were prepared in two variants for each type of target (Zr, Cu, Ti and AgCu) with different power settings, respectively 0.4 and 0.9 kW. The subsequent labelling of the samples is according to the target used and the performance of the device during the deposition process (Tab. 1).

Tab. 1 *Power parameters during the deposition*

Sample marked	AgCu0.9	AgCu0.4	Cu0.9	Cu0.4	Ti0.9	Ti0.4	Zr0.9	Zr0.4
Target	AgCu	AgCu	Cu	Cu	Ti	Ti	Zr	Zr
Power (kW)	0.9	0.4	0.9	0.4	0.9	0.4	0.9	0.4

2.3 Thickness of thin layers

The thickness of the thin layers was monitored during the deposition process using a crystal monitor (QCM method), which was attached to the chamber and its software.

2.4 Pore size and chemical composition

The structure of the sample surfaces and filter pores were analysed using scanning electron microscopy on a Carl Zeiss ULTRA Plus microscope. The pore diameter was evaluated using image analysis in Matlab software (The MathWorks, Inc.).

The chemical composition of AgCu thin layers was evaluated using scanning electron microscopy on Carl Zeiss ULTRA Plus microscope with EDS analysis.

2.5 Height parameters of surface roughness

The morphology, topography, and surface roughness were evaluated using a non-contact optical 3D profilometer S Neox from SENSOFAR according to the *ISO 4287:1997 standard*. The data were averaged from three measurements in different areas of the filter surface. The average arithmetic height of the surface (*Sa*), the kurtosis (*Sku*), and the maximum height of the surface (*Sz*) were monitored. Based on the values of the kurtosis was determined the sharpness of the profile – biased above the mean plane (*Sku*<3), normal distribution (*Sku*=3), and spiked (*Sku*>3). These parameters are crucial for the material properties, such as thin layers of adhesion to the substrate or reducing biofilm formation. [10, 11]

2.6 Tribological analysis

The tribological properties of the modified surfaces, which describe the filter surface's resistance to damage/wear, were investigated using a TRB³ tribometer from Anton Paar before and after the application of thin layers. The *Ball-on-Flat* method with linear reciprocating motion of the counter-body (ball: Soda Lime material, diameter 6.00 mm, KNOOP-KHN hardness: 465; specific gravity: 2.500 g/cm³ from Redhill Precision company) was used against the tested materials according to the *ASTM G133* standard. The experimental parameters used were a table movement speed of 4.5 cm/s, a counter body load of 0.5 N, and a travelled distance of 5 m. The values of the static and dynamic coefficient of friction were obtained on each of the investigated surfaces.

The tribological trace (depth and width of the damaged material) was characterized using a non-contact optical 3D profilometer S Neox from SENSOFAR, averaged from six measurements [12, 13].

2.7 Resistance to deformation

The resistance to deformation was evaluated using the stiffness test for flat textiles according to the *ČSN 80 0858 standard* on a TH-5 stiffness tester. Samples were 2.5 cm × 4.7 cm, securing the sample in two directions, a thin layer towards the device and away from it. The samples were prepared according to

standards ČSN 80 0069 and ČSN 80 0072. The bending stress was applied by deflecting the tester jaws at an angle of 60°. Three measurements were performed with the sample placed in the jaws, with the layer facing both sides, since the thin layers were deposited on one side of the filtration material.

2.8 Contact angle and surface energy

The contact angle and the surface energy were determined using the Drop test method by the Surface Energy Evaluation System. In this test, a drop of distilled water with a volume of 3 µl was applied to the sample. The contact angle was measured by the software, and the surface energy was calculated according to the Li-Neumann model. The value of surface energy (g), its negative deviation (Sg-), and positive deviation were determined (Sg+). Based on the contact angle values, it was determined whether the liquid wets (angle from 0° to 90°) or does not wet (angle from 90° to 180°) the surface. According to the surface energy values, its degree was determined - high (above 300 mJ/m², wets the surface), medium (from 36 mJ/m² to 300 mJ/m²), and low (below 36 mJ/m², does not wet the surface). These parameters define whether the samples have hydrophilic or hydrophobic surfaces. Ten measurements were taken on each sample.

2.9 Filter permeability

To evaluate the permeability of the filters, a 20 ml solution containing particles with the size of around 1.0-2.0 µm or 0.5-1.0 µm was filtered using a PSF NALGENE filtration setup (P-LAB a.s.) with the pump (Laboport KNF N86, with 160 mbar) and the time was measured during the tests. The solution was prepared from 400 ml of physiological saline and 4 ml of particle suspension with a concentration corresponding to 0.15 mol/l.

3 Results

3.1 Thickness of thin layers

Based on the thickness values (Tab. 2), thin layers applied at a power of 0.9 kW exhibited greater thickness than those deposited at 0.4 kW.

Tab. 2 *Thickness of thin layers*

Sample marked	AgCu0.9	AgCu0.4	Cu0.9	Cu0.4	Ti0.9	Ti0.4	Zr0.9	Zr0.4
Thickness (nm)	40	13	20	8	4	2	4	3

3.2 Pore size and chemical composition

The structure of the sample surfaces is shown in Fig. 1. No significant reduction in the pore size was observed.

The substrate exhibited a structure with a rugged surface forming a web with visible pores. As shown in Figure 1, the AgCu0.9 sample has a more uniform surface than the nylon filter substrate, with smoother pore edges. In comparison, the AgCu0.4, Cu0.9, and Cu0.4 samples show surfaces that are very similar to the nylon filter, although their pore edges appear slightly smoother. The thin films deposited from titanium and zirconium targets also show a surface structure similar to the substrate.

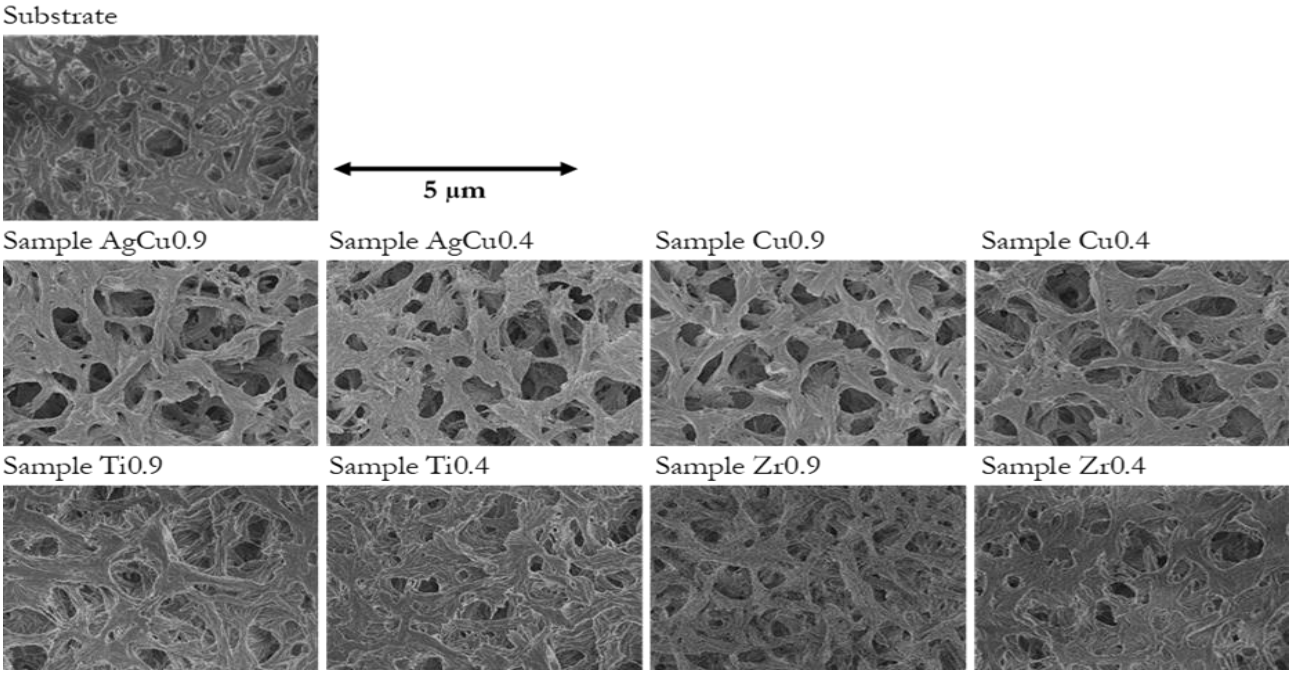

Fig. 1 *SEM images of substrate and samples with thin layers*

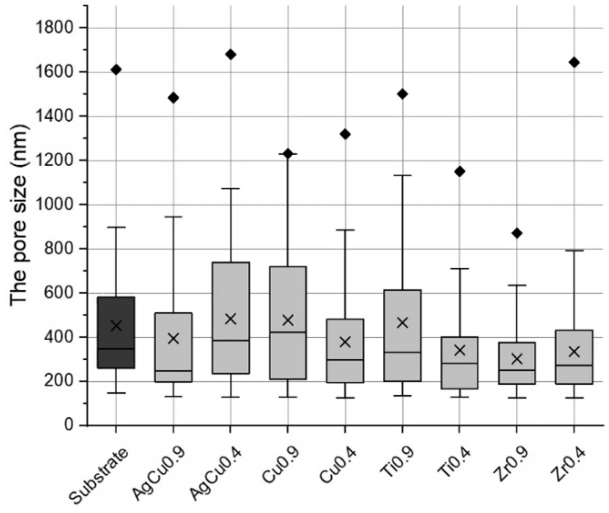

Fig. 2 *The pore size of filters*

The pore size evaluation (Fig. 2) was conducted to demonstrate whether the deposition of the filter with thin layers does not cause a restriction in porosity, which may result in a reduction in gas or liquid flow. The evaluated pore diameters of the modified filtration materials are shown in the Box-plot in Figure 2. Marks outside the box plot correspond to outliers; the cross represents the average value, and the line inside the box is the median value. The difference between the mean and median indicates that the evaluated data are not normally distributed.

Based on the measured values of the chemical composition, the Ag:Cu atomic ratio was determined to be 58:42 (AgCu0.4) and 59:41 (AgCu0.9).

3.3 Height parameters of surface roughness

The measured values of the parameter *Sa* for the samples AgCu0.4, Cu0.4, and Zr0.4 (Fig. 3a) are significantly lower than for the base material. The *Sku* values (Fig. 3b) of sample AgCu0.9 exhibited a wide range, with higher values measured in sample AgCu0.4 and lower in sample Ti0.9 than the substrate. A wide range of *Sz* values (Fig. 3c) was detected in sample AgCu0.9.

On the investigated surfaces, the profile sharpness was monitored according to the results on the Box-plot graphs (Fig. 3b). For the base material, the Normal distribution was evaluated; for the samples AgCu0.9, AgCu0.4, Ti0.4, Zr0.9 and Zr0.4 the distribution profile sharpness was spiked; for Cu0.9 and Cu0.4 samples Normal distribution/Spiked and for Ti0.9 sample – distribution biased above the mean plane.

The surface images of the filter material samples captured by a confocal microscope are shown in Figure 4.

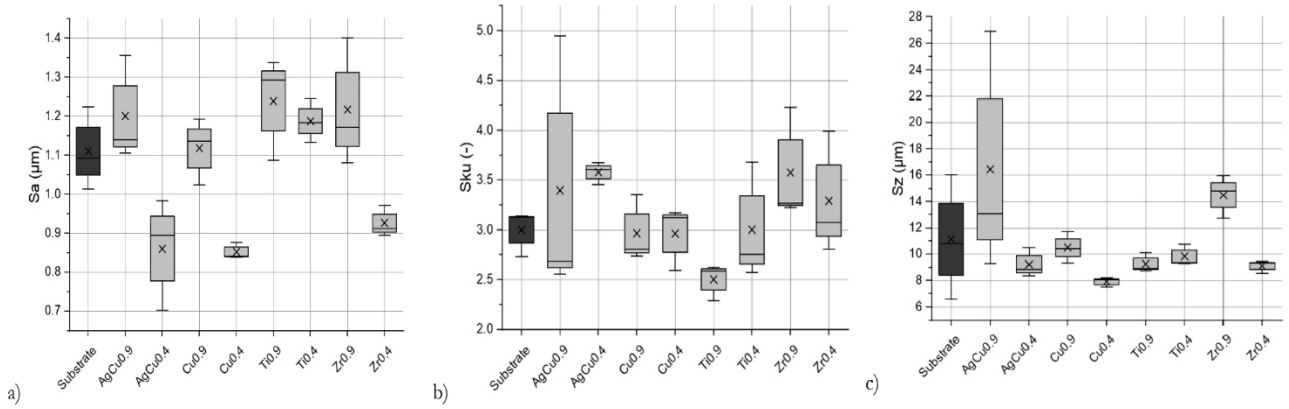

Fig. 3 *Height parameters of surface roughness: a) the average arithmetic height of the surface; b) the kurtosis, and c) the maximum height of the surface*

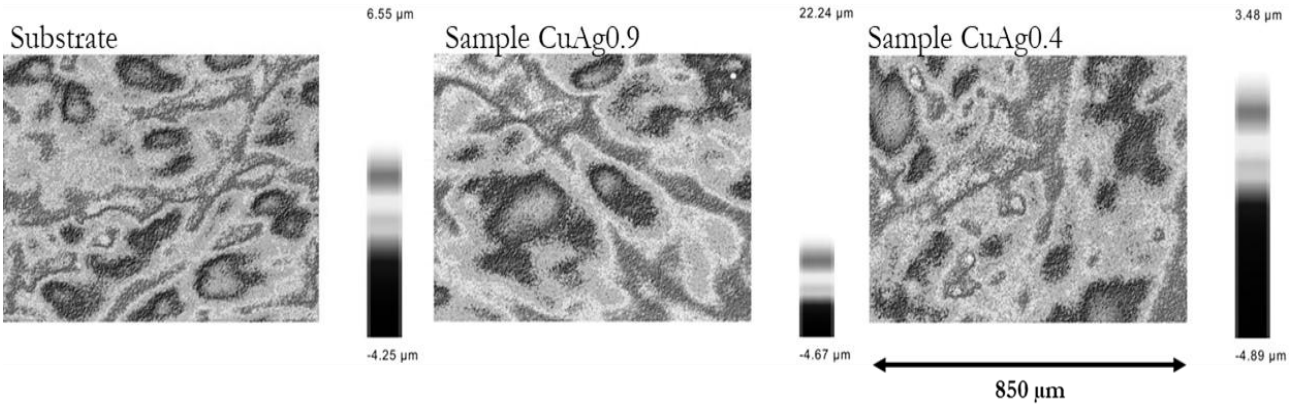

Fig. 4 *Representative images of the sample profile captured at 20× objective magnification*

3.4 Tribological analysis

Table 3 presents the values of the static and dynamic coefficient of friction. For the substrate and samples AgCu0.9, AgCu0.4, and Cu0.9, the static friction coefficient of friction was lower than the average dynamic coefficient value. For the other samples, the static friction coefficient value was higher or equal to the average dynamic friction coefficient value. A decrease in the dynamic coefficient of friction was found for all coated samples compared to the base material.

The depths of the tribological track showed high values for samples AgCu0.4 and Cu0.4 compared to the substrate (Fig. 5a). These values had a wide range (different parts of the tribological track differed from each other). The width of the track for all samples, except Ti0.4 and Zr0.9, had a wide range of values, and an increase in measured values was detected for samples AgCu0.4, Cu0.9, Cu0.4, and Ti0.9 (Fig. 5b).

Thin layers deposited at a power of 0.9 kW exhibited greater thin layer thickness and lower static friction coefficient values than the layers deposited at 0.4 kW, except those for the element titanium.

Tab. 3 *Measured values of friction coefficients and standard deviations of the dynamic coefficient*

Sample	Static coefficient of friction μ_{stat} (-)	Dynamic coefficient of friction μ_{kin} (-)
Substrate	0.74	0.82 ± 0.11
AgCu0.9	0.26	0.66 ± 0.10
AgCu0.4	0.46	0.59 ± 0.07
Cu0.9	0.43	0.69 ± 0.08
Cu0.4	0.70	0.61 ± 0.07
Ti0.9	0.79	0.67 ± 0.05
Ti0.4	0.72	0.72 ± 0.07
Zr0.9	0.74	0.56 ± 0.05
Zr0.4	0.77	0.64 ± 0.06

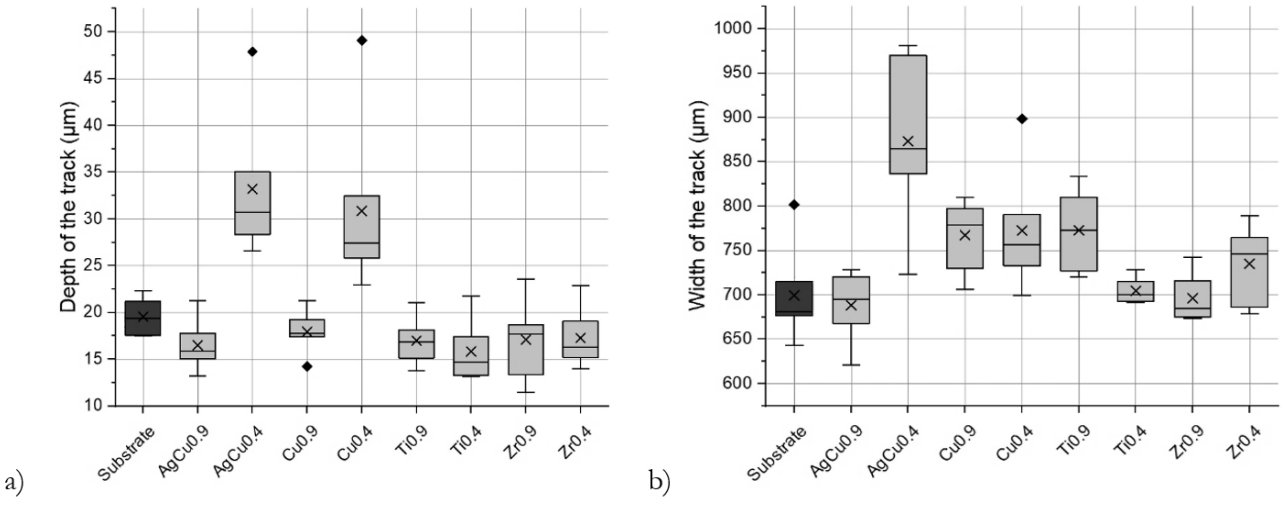

Fig. 5 *Characterization of the tribological trace a) depth of the tribology testing track and b) width of the tribology testing track*

3.5 Resistance to deformation

The results were obtained with the sample placed in the jaws, with the layer facing both sides (Fig. 6a and Fig. 6b). The bending moment values of the thin layers in the direction away from the device were higher than the substrate for all samples except Cu0.4 (Fig. 6b), and the bending moment values of the layers towards the device were higher than the substrate for all samples except Cu0.4 and Zr0.9 (Fig. 6a). According to Figure 6, the values for the sample Cu0.4 were measured within a narrow range. The bending moment of the modified materials is almost always higher than that of the substrates (nylon filter).

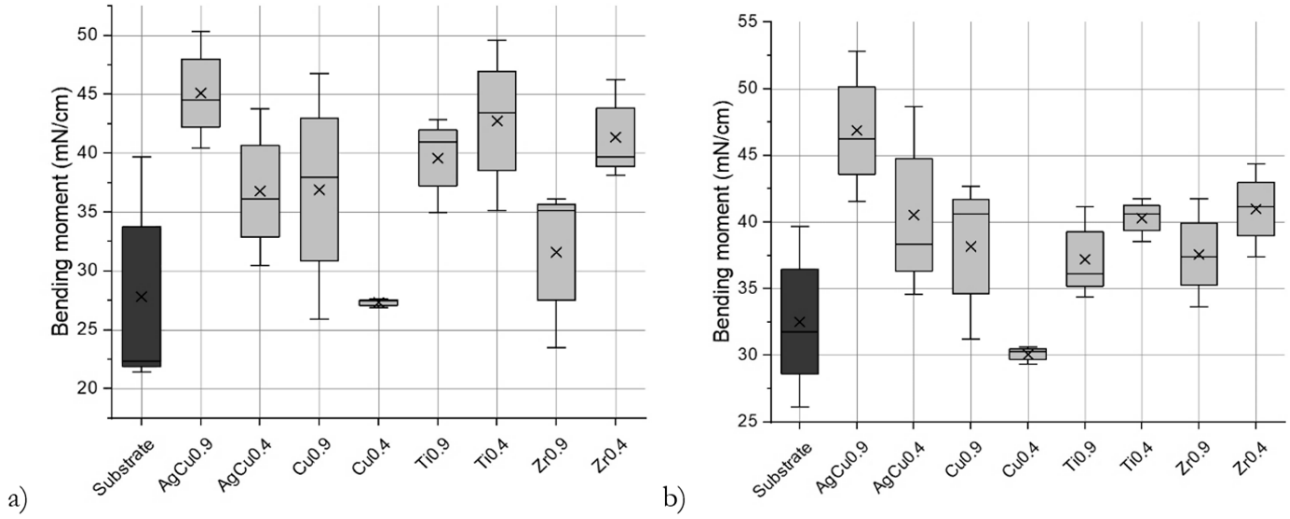

Fig. 6 *Bending moment of samples during layer testing a) towards the device and b) away from the device*

3.6 Contact angle and surface energy

The results of the contact angle are shown in Figure 7, and the results of surface energy are presented in Table 4. The substrate is characterized by low contact angle values and a medium level of surface energy, i.e., it has a hydrophilic surface. For all samples with thin layers, a larger contact angle and lower surface energy were measured than on the substrate, the exception is the Zr0.9 sample (Fig. 7). The substrate exhibits a hydrophilic character (contact angle of 23°), while only one modified sample (Zr0.9) was classified as hydrophilic (contact angle 28°), see Figure 7. All other modified surfaces show hydrophobic properties.

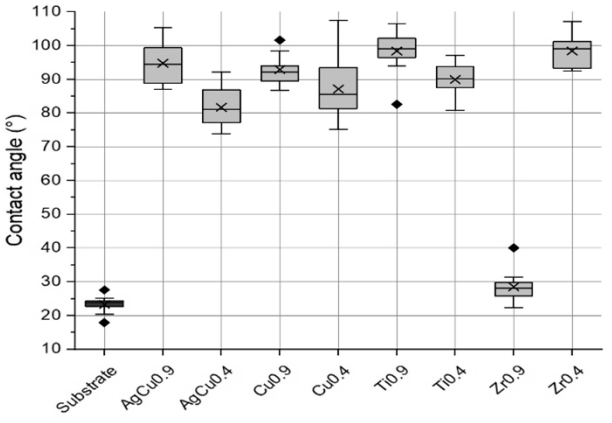

Fig. 7 *Contact angle measured values*

Tab. 4 *Surface energy and hydrophilic or hydrophobic type of surface*

Sample	Wet/Does not wet the surface	g (mJ/m²)	Sg- (mJ/m²)	Sg+ (mJ/m²)	Surface energy	Hydrophilic/ Hydrophobic surface
Substrate	Wet	67.45	1.90	2.08	Medium	Hydrophilic
AgCu0.9	Wet/Does not wet	25.27	7.29	4.24	Low	Hydrophobic
AgCu0.4	Wet/Does not wet	35.00	7.08	5.84	Low/Medium	Undefined
Cu0.9	Wet/Does not wet	27.83	5.62	4.67	Low	Hydrophobic
Cu0.4	Wet/Does not wet	30.28	14.24	8.82	Low/Medium	Undefined
Ti0.9	Does not wet	24.06	4.57	10.59	Low	Hydrophobic
Ti0.4	Wet/Does not wet	29.39	4.55	6.56	Low	Hydrophobic
Zr0.9	Wet	64.85	2.89	1.83	Medium	Hydrophilic
Zr0.4	Does not wet	24.06	5.08	2.80	Low	Hydrophobic

3.7 Filter permeability

For the permeability of filters using a solution with a particle size of 1.0-2.0 μm, an extending filtration time compared to the substrate was detected for all samples (Tab. 5). The results of the permeability of filters with a solution with a particle size of 0.5-1.0 μm for samples Cu0.4 and Zr0.4 were similar to the substrate, while for samples AgCu0.9, AgCu0.4, and Zr0.9, a higher time. The filtration time measured was longer compared to the original unmodified filter, on average, by approximately 30%. For the samples Ti0.9 and Ti0.4, a lower time compared to the substrate was measured (Tab. 5).

Tab. 5 *Filtration time of solutions*

Sample	Substrate	AgCu0.9	AgCu0.4	Cu0.9	Cu0.4	Ti0.9	Ti0.4	Zr0.9	Zr0.4
Time (s) 1.0-2.0 μm	6.9	13.2	7.6	10.0	12.2	7.8	7.6	8.0	8.6
Time (s) 0.5-1.0 μm	6.8	7.6	7.3	10.1	7.0	6.4	6.3	7.2	6.9

4 Discussion of results

Based on the measured values, it was found that the thickness of the thin layers increases with higher source power, which depends on the sputtering yield (Y), which is written in articles [14] and [15]. The results show the highest sputtering rate for copper-silver alloy, followed by copper, and the lowest for titanium and zirconium, as demonstrated in the article [16].

Based on the SEM analysis (Fig. 1), all thin layers remain well attached to the sample surfaces, with no signs of delamination observed. Adhesion of thin films is commonly evaluated using the scratch test [17]; however, this method is not suitable for nylon filter substrates and was therefore not used in this study. The deposited layers do not obstruct or fill the pores of the substrates, and the porosity of the original substrate is not significantly reduced by the coating process. At a greater layer thickness (Table 2, e.g. Sample AgCu0.9), the surface structure became smoother, while the pore geometry remained stable, with no apparent enlargement or interconnection. Thin layers of metals and alloys of Cu, Ti, Zr and AgCu targets are smooth (Fig. 3c), without apparent relief, as confirmed by articles [18] and [3]. In most samples, there is a slight reduction in pore size. This is most likely caused by the thermal effect on nylon, whose sharp edges retract in response to temperature. The exception is the AgCu0.9 sample, where the thickness of the deposited layer is the largest (40 nm, see Table 2). The large range of measured values may be due to deformation of the underlying material due to the layer thickness and deposition temperature. The reduction in pore size after the deposition of the thin layers was also described in articles [19] and [7]. These articles mention a slight decrease in pore size and the same pore area coverage for thin layers up to a thickness of 50 nm.

The selection of the scanned area influences the height parameters of the surface roughness of filters. The surface of the substrate is rugged. It is the reason that most measured samples show a wide interquartile range for *Sa* values (Fig. 3a). A connection between *Sku* and *Sz* values was detected, where increasing *Sku* values correspond to increasing *Sz* values (Fig. 3b and 3c). Article [20] describes this connection that *Sku* is directly related to the heights of peaks and depths of valleys. Based on the Sku values, which are close to 3 (from 2.29 to 4.23), it can be concluded that the height distributions of surfaces of the samples, except AgCu0.9, approximate a normal distribution. There is no wide range between individual layers at different source powers, which proves that these layers have similarly distributed sharpness in the structure. This trend is described in article [21], which states that for most samples with thin Ti-based layers, the Sku values were within a similar range (from 3.22 to 4.44) regardless of surface pretreatment.

For the AgCu0.9 layer, significantly higher bending moment values than other samples were recorded (Fig. 6). This observation suggests that the increased thickness of the AgCu0.9 layer (40 nm) may contribute to the enhanced bending moment, potentially due to improved mechanical integrity, greater resistance to deformation, or stronger interaction with the substrate. It was found that the substrate has hydrophilic properties, and samples with thin layers exhibit more hydrophobic properties (Figure 7, Table 4). Article [20] reports a reduction in surface energy for samples with deposited AgCu layers compared to the PP (polypropylene) substrate, which was also confirmed in this work. The article [22] discusses the dependence of the hydrophobic behaviour of materials on source power, where it was found that at higher source power, the material with a thin layer exhibits more hydrophobic properties. This was detected in sample AgCu0.9, which has hydrophobic properties, and sample AgCu0.4, which is on the borderline between hydrophilicity and hydrophobicity.

For AgCu and Cu layers, a higher static coefficient of friction was detected for samples using lower source power, and the track depth was deeper than that of the substrates (Tab. 3). The tribological tracks of samples AgCu0.4 and Cu0.4 show extensive damage, see Figure 8. The greater depth of damage to the filter surface was measured for both samples (Fig. 5a), which may be caused by poor adhesion of the layers to the base material.

Table 5 shows no significant increase in filtration time for samples with deposited thin layers compared to the bare substrate when using the solution containing smaller particles (0.5–1.0 μm). In contrast, for the filtrate with larger particles (1.0–2.0 μm), a reduction in solution flow rate was observed in samples with greater thickness of thin layers, most notably in AgCu0.9, Cu0.9, and Cu0.9. Article [8] states that nonwoven fabric with a 5 nm AgCu layer exhibits high filtration efficiency, demonstrating that effective filtration is achieved even with deposited thin layers. This is further supported by the results we obtained using the solution with smaller particles.

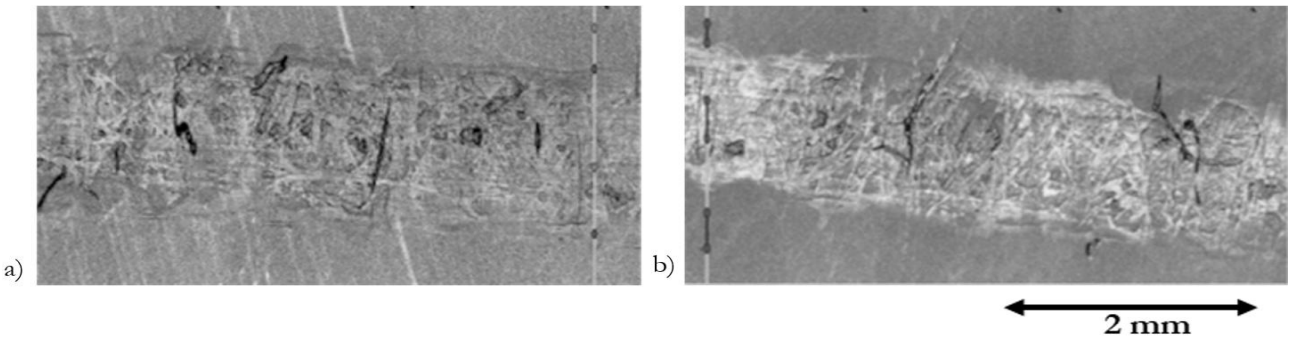

Fig. 8 *Tribological track damage in a) AgCu0.4 and b) Cu0.4 samples*

5 Summary

The research verifies the possibilities of using magnetron deposition of thin layers on filters made of nylon (polyamide 6.6) using AgCu, Cu, Zr, and Ti targets. The surface modification of the filters did not significantly change the samples' resistance to deformation; however, a significant effect on surface wettability was demonstrated (from the original contact angle values of 23° to values around 90°). For samples of pure metals (Cu, Ti, and Zr), no significant reduction in pore size was observed. Layers deposited at a source power of 0.9 kW achieve greater thickness and simultaneously lower static friction coefficients than at 0.4 kW. Greater layer thickness did not prolong filtration time for filtering the solution containing smaller particles (0.5–1.0 μm) in comparison with the thinner layer.

Further research will address potential structural changes over a longer time horizon, e.g., after 12 months. The samples will be subjected to cyclic bending stress, which better simulates the influence of the real environment. A leachability test will be conducted to confirm whether the layers may release particles/elements into the surrounding environment, and antibacterial tests will be performed repeatedly to verify the duration of antibacterial efficacy, i.e., the number of filtration cycles.

Acknowledgment

This publication was supported by the Student Grant Competition of the Technical University of Liberec within the project SGS-2025-5534. This publication was written at the TUL with the support of the Institutional Endowment for the Long-Term Conceptual Development of Research Institutes, as provided by the MSMT of the Czech Republic 2025.

References

[1] WANG L., HU CH., SHAO L.. The antimicrobial activity of nanoparticles: present situation and prospects for the future. *International Journal of Nanomedicine*. February 2017. Vol. Volume 12, p. 1227–1249. DOI 10.2147/IJN.S121956.

[2] ETIEMBLE, A., DER LOUGHIAN, C., APREUTESEI, M., LANGLOIS, C., CARDINAL, S., PELLETIER, J.M., PIERSON, J.-F., STEYER, P. Innovative Zr-Cu-Ag thin film metallic glass deposed by magnetron PVD sputtering for antibacterial applications. *Journal of Alloys and Compounds*. June 2017. Vol. 707, p. 155–161. DOI 10.1016/j.jallcom.2016.12.259.

[3] MIHUT D. M., AFSHAR A., LACKEY L. W., LE K. N.. Antibacterial effectiveness of metallic nanoparticles deposited on water filter paper by magnetron sputtering. *Surface and Coatings Technology*. 25 June 2019. Vol. 368, p. 59–66. DOI 10.1016/j.surfcoat.2019.04.039.

[4] RTIMI S., DIONYSIOU D. D., PILLAI S. C., KIWI J.. Advances in catalytic/photocatalytic bacterial inactivation by nano Ag and Cu coated surfaces and medical devices. *Applied Catalysis B: Environmental*. January 2019. Vol. 240, p. 291–318. DOI 10.1016/j.apcatb.2018.07.025.

[5] BALLO M. K. S., RTIMI S., MANCINI S., KIWI J., PULGARIN C., ENTENZA J. M., BIZZINI A.. Bactericidal activity and mechanism of action of copper-sputtered flexible surfaces against multidrug-resistant pathogens. *Applied Microbiology and Biotechnology*. July 2016. Vol. 100, no. 13, p. 5945–5953. DOI 10.1007/s00253-016-7450-7.

[6] AKHIDIME I. D., SAUBADE F., BENSON P. S., BUTLER J. A., OLIVIER S., KELLY P., VERRAN J., WHITEHEAD K. A.. The antimicrobial effect of metal substrates on food pathogens. *Food and Bioproducts Processing*. January 2019. Vol. 113, p. 68–76. DOI 10.1016/j.fbp.2018.09.003.

[7] COELHO L. L., GRAO M., POMONE T., RATOVA M., KELLY P., WILHELM M., MOREIRA R. de F. P. M.. Photocatalytic microfiltration membranes produced by

magnetron sputtering with self-cleaning capabilities. *Thin Solid Films*. 1 April 2022. Vol. 747, p. 139143. DOI 10.1016/j.tsf.2022.139143.

[8] HUANG X., HU Q., LI J., YAO W., WANG CH., FENG Y., SONG W.. Sputtering-Deposited Ultra-Thin Ag–Cu Films on Non-Woven Fabrics for Face Masks with Antimicrobial Function and Breath NOx Response. *Materials*. 29 March 2024. Vol. 17, p. 1574. DOI 10.3390/ma17071574.

[9] Laboratory equipment | Fisher Scientific. Fisher Scientific. Online. [Accessed 3 March 2024]. Available from: https://www.thermofisher.cz/.

[10] BAKALOVA T., PETKOV N., BAHCHEDZHIEV H., KEJZLAR P., LOUDA P.. Comparison of Mechanical and Tribological Properties of TiCN and CrCN Coatings Deposited by CAD. *Manufacturing Technology*. 1 October 2016. Vol. 16, no. 5, p. 854–858. DOI 10.21062/ujep/x.2016/a/1213-2489/MT/16/5/854.

[11] BLUNT L., JIANG X.. *Advanced techniques for assessment surface topography : development of a basis for 3D surface texture standards "surfstand."* . London : Kogan Page Science, [no date]. ISBN 1-4175-2637-8.

[12] BAKALOVA T., LOUDA P., VOLESKÝ L., ANDRŠOVÁ Z.. The use of optical microscopy to evaluate the tribological properties. *Manufacturing Technology*. 1 October 2014. Vol. 14, no. 3, p. 256–261. DOI: 10.21062/ujep/x.2014/a/1213-2489/MT/14/3/256.

[13] KRAFKA M., LEMBERK L., PETKOV N., SVOBODOVÁ L., BAKALOVA T.. Comparison of Mechanical and Tribological Properties of TiN and ZrN Coatings Deposited by Arc-PVD. *Manufacturing Technology*. 4 May 2023. Vol. 23, no. 2, p. 194-203, DOI: 10.21062/mft.2023.029.

[14] KAVITHA A., KANNAN R., RAJASHABALA S. Effect of target power on the physical properties of Ti thin films prepared by DC magnetron sputtering with supported discharge. *Materials Science*-Poland. 24 February 2017. Vol. 35, no. 1, p. 173–180. DOI 10.1515/msp-2017-0022. 13.

[15] LE, M.-T., SOHN Y.-U., LIM J.-W., CHOI G.-S.. Effect of Sputtering Power on the Nucleation and Growth of Cu Films Deposited by Magnetron Sputtering. *MATERIALS TRANSACTIONS*. 2010. Vol. 51, no. 1, p. 116–120. DOI 10.2320/matertrans.M2009183.

[16] MAHNE N., ČEKADA M., PANJAN, M.. Total and Differential Sputtering Yields Explored by SRIM Simulations. *Coatings*. 13 October 2022. Vol. 12, p. 1541. DOI 10.3390/coatings12101541.

[17] BAKALOVA T., PETKOV N., BAHCHEDZHIEV H., KEJZLAR P., VOLESKÝ L.. Monitoring Changes in the Tribological Behaviour of CrCN Thin Layers with Different CH_4/N_2 Gas Ratios at Room and Elevated Temperatures. *Manufacturing Technology*. 1 September 2018. Vol. 18, no. 4, p. 533–537. DOI 10.21062/ujep/133.2018/a/1213-2489/MT/18/4/533. T16.

[18] LAN M., LI H., WANG D., LI Y., XU G.. Fabrication of glass fibers uniformly coated with metal films by magnetron sputtering by a two step process involving fixation by a photoresist. *Vacuum*. 30 November 2014. Vol. 110, p. 87–93. DOI 10.1016/j.vacuum.2014.09.003.

[19] KASSA S. T., HU CH.-CH., LIAO Y.-CH., CHEN J.-K., CHU J. P. Thin film metallic glass as an effective coating for enhancing oil/water separation of electrospun polyacrylonitrile membrane. *Surface and Coatings Technology*. 25 June 2019. Vol. 368, p. 33–41. DOI 10.1016/j.surfcoat.2019.04.030.

[20] VAEZZADEH ASADI M., SOLOOKINEJAD G., IZADNESHAN H.. Structural, Morphological and Optical Analysis of TiO_2 Thin Films Prepared by RF Magnetron Sputtering. *Journal of Optoelectronical Nanostructures*. 2021. Vol. 6, no. 4, p. 59–94. DOI 10.30495/jopn.2021.28681.1230.

[21] ZHURAVLEVA I., SUROVTSEVA M., VAVER A., SUPRUN E., KIM I., BONDARENKO N., KUZMIN O., MAYOROV A., POVESHCHENKO O.. Effect of the Nanorough Surface of TiO2 Thin Films on the Compatibility with Endothelial Cells. *International Journal of Molecular Sciences*. 3 April 2023. Vol. 24, p. 6699. DOI 10.3390/ijms24076699.

[22] CHU CH., HU, X., YAN H., SUN Y.. Surface functionalization of nanostructured Cu/Ag-deposited polypropylene fiber by magnetron sputtering. *e-Polymers*. 29 January 2021. Vol. 21, p. 140–150. DOI 10.1515/epoly-2021-0020.